Fracture Mechanics of Concrete Structures,
Proceedings FRAMCOS-2, edited by Folker H. Wittmann,
AEDIFICATIO Publishers, D-79104 Freiburg (1995)

MULTIFRACTAL SCALING LAW FOR THE FRACTURE ENERGY VARIATION OF CONCRETE STRUCTURES

A. Carpinteri and B. Chiaia,
Department of Structural Engineering, Politecnico di Torino
10129 Torino, Italy

Abstract
The phenomenon of the size-dependence of the concrete fracture energy is discussed. It is shown that the scaling of toughness can be consistently interpreted by means of a fractal model, the influence of microstructural disorder being predominant. Moreover, at the larger scales, the fields homogeneization progressively comes into play, leading to the multifractal scaling of the physical properties. A Multifractal Scaling Law (MFSL) is proposed for the fracture energy $\mathcal{G}_F$, following the MFSL already applied to the scale-dependence of strength (Carpinteri et al., 1994). By means of best-fitting of the test data, the full range of the scaling is described and an asymptotic value of $\mathcal{G}_F$, valid for real-sized structures, can be determined.

1 Introduction: disorder, fracture energy and size effects

The constitutive model that appears more suitable for describing the tensile behavior of heterogeneous materials like concrete, ceramics and rocks is the Cohesive Crack Model by Hillerborg et al. (1976), which is based on two different relationships (Fig. 1a). The first one is the elastic-plastic *stress-strain* law, holding up to the ultimate tensile stress σ_u, and the second is a *stress-crack opening displacement* law, also called the *cohesive* *law*, which describes the softening behavior provided by the damaged process zone.

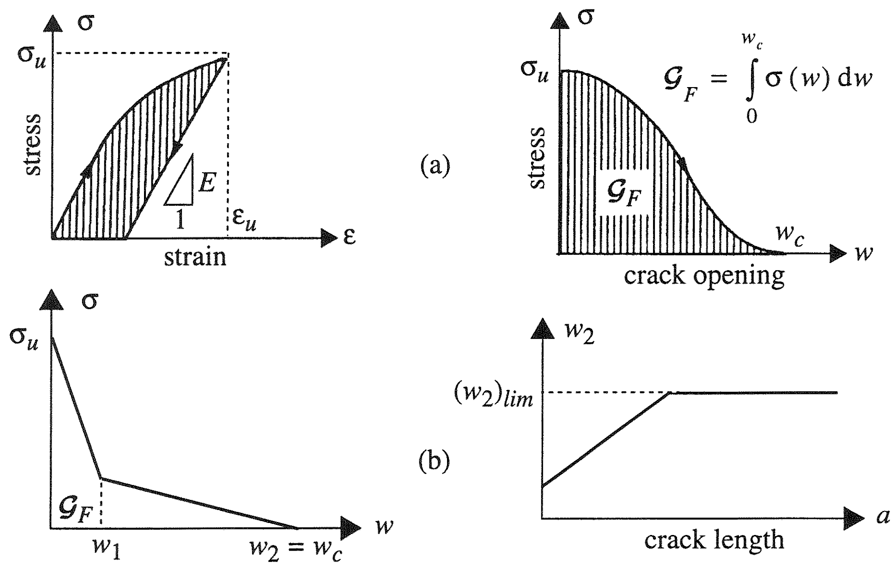

Fig. 1. Cohesive crack model (a) and FPZ evolution (b) during crack propagation (Hu & Wittmann, 1992).

The area under the *cohesive law* $\sigma(w)$ represents the energy dissipated on the unitary crack surface and, by definition, is called the *fracture energy* $\mathcal{G}_F$ of the material:

$$\mathcal{G}_F = \frac{W_F}{A_{lig}}, \tag{1}$$

where W_F is the *total* work necessary for the complete fracture of the specimen and A_{lig} is the area of the initial resisting ligament. The cohesive law is generally assumed as a material characteristic, since it intimately depends on the microstructure and on the dissipation mechanisms involved in the fracture process (bridging, creep, aggregate interlocking): therefore, the fracture energy $\mathcal{G}_F$ is usually assumed as a material constant.

The experimental determination of concrete fracture energy $\mathcal{G}_F$ is nowadays ruled by a RILEM Recommendation (1985) and consists in a standard displacement-controlled three-point bending test. A huge number of tests preceded and followed the publication of the aforementioned Recommendation: unfortunately, the increase of the measured value of $\mathcal{G}_F$ with increasing specimen size has often been detected, which is essentially the same trend observed in the case of other toughness parameters (K_{IC} or *J-integral*), even in different materials. In the first extensive round-robin almost 700 beams were tested in 14 different laboratories, but the size range was rather small: after analyzing the results, Hillerborg (1985) concluded that $\mathcal{G}_F$ could be considered as a material constant, being its variation with size less than one third of the corresponding variation of strength. Subsequent investigations by Swartz & Refai (1987) on wider size ranges showed that the $\mathcal{G}_F$ variation with size is not negligible at all, and that this scaling effect has to be considered so important as the more familiar size effect on tensile strength.

Hu & Wittmann (1992) state that responsible for the variation of the nominal fracture energy $\mathcal{G}_F$ is the increase with size of the fracture process zone (FPZ) width a_p, which causes the increase of the critical crack opening displacement $w_2=w_c$ in a bilinear cohesive law (Fig. 1b). Since the energy dissipation takes place in the fracture process zone, whose width expands during crack propagation (R-curve behavior) at least up to a limit value (*fully-developed process zone*), it is reasonable to suppose that in larger specimens, where the FPZ can develop entirely, a higher value of w_c is reached, yielding a higher measured fracture energy. A *local fracture energy* $g_F(x)$ is proposed, proportional to the FPZ width and thus to w_c, whose integration along the fracture path provides a size-dependent fracture energy, according to the experimental trend. Beyond a threshold structural size, the FPZ attains its highest width and remains constant: an asymptotic value of $\mathcal{G}_F$ is thus measured in the limit of the largest sizes.

Three causes, not adequately taken into account by the RILEM standard test, are considered by Elices et al. (1992) to be responsible for the variation of $\mathcal{G}_F$ with size: the energy dissipation from hysteresis in the testing equipment and in the lateral supports, the bulk dissipation in the most stressed regions of the sample and the dissipated energy at the end of the loading process, which is neglected due to the cutting of the P-δ tail.

Starting from its definition, the fracture energy $\mathcal{G}_F$ does not represent a *local* toughness parameter, like the critical stress-intensity factor K_{IC} (*tensional fracture toughness*); it rather represents a *mean-field* quantity, involving the whole complexity of microscopical phenomena ahead of the crack tip, which take part in the *total* work-of-fracture (*energy fracture toughness*). The great advantage of such a *global* parameter is provided by the absence of linearity requirements in the fracture process: no information on the singular stress field at the crack tip is needed, and Linear Elastic Fracture Mechanics can be neglected. On the other hand, the physical meaning of $\mathcal{G}_F$ reveals to be ambiguous, being it defined, according to Eq. (1), as a purely surface energy ($[F][L]^{-1}$). On the contrary, it refers to a much more complicated process of dissipation, taking place in a *higher dimensional space* which includes all the previously mentioned micromechanisms of damage (Carpinteri, 1994a).

2 Evidence of fractality in the fracture of concrete

All the constitutive models developed to study the mechanical properties of heterogeneous materials have to be strictly connected to a particular scale of observation (Fig. 2). In particular, the progressive vanishing of the influence of disorder as the scale increases must be taken into account.

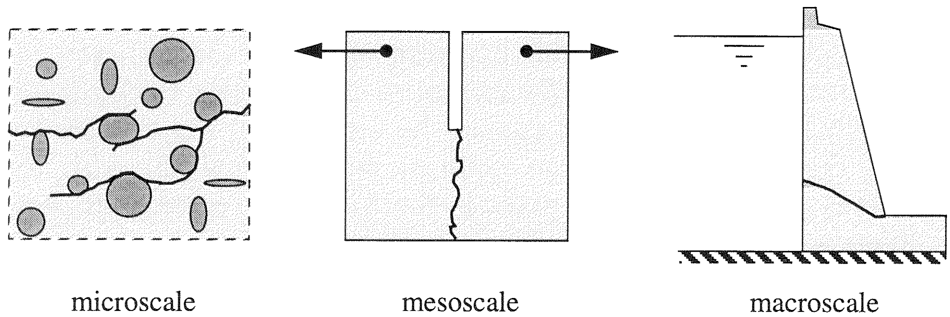

Fig. 2. Multi-scale propagation of fracture in concrete.

In the case of concrete, for example, micromechanical models apply at the scale of the aggregates, where debonding at the matrix interface, bridging and overlapping have to be considered. Numerical simulations performed by Schlangen (1995) show that, at this scale, local rotations play a fundamental role in the fracture behavior, and therefore the Cosserat continuum yields a more realistic description of the material. On the other hand, at the macroscopic level of the real structures, fracture develops in a *global* manner, resembling that of more homogeneous materials, the influence of disorder resulting much weaker.

The question naturally arises whether a common feature relating the various scales of observation can be established in order to describe the full scaling range of the mechanical properties. The application of Fractal Geometry to cementitious materials, although relatively recent with respect to the case of rocks and metals, represents an appropriate approach in this sense, due to the *multi-scale heterogeneity* of these composites.

Statistical *self-similarity* (the property of sets showing statistically similar morphologies at various scales of observation) has nowadays been extensively detected in the case of concrete fracture patterns (Carpinteri & Chiaia, 1995). The hierarchical propagation of cracks, in fact, reflects the hierarchical microstructure of concrete, which ranges from the microscopic level of the cement clinker up to the macroscopic level of the coarse aggregates embedded in the paste. The first experimental application of the fractal concepts to concrete fracture surfaces is that of Saouma et al. (1990), who detected anomalously low values of the fractal dimension Δ

due to the multifractal character of the considered domains. Lange (1993), Issa & Hammad (1994) and Carpinteri & Chiaia (1995) investigated on concrete fracture surfaces by means of different experimental techniques, always proving the fractality or better, the *multifractality*, of the fracture domains.

The main aspect to be highlighted, beyond the phenomenological evidence, is the physical significance of fractality. The deep connection between Physics and Topology is nowadays well known in the framework of critical phenomena. All the physical systems undergoing catastrophic transformations, like phase transitions, earthquakes and brittle fracture, show at the critical point fluctuations that are *self-similar* at all length scales, thus resulting in the (theoretical) absence of any internal characteristic length (or, which is the same, in the *infinite correlation length* of the phenomenon).

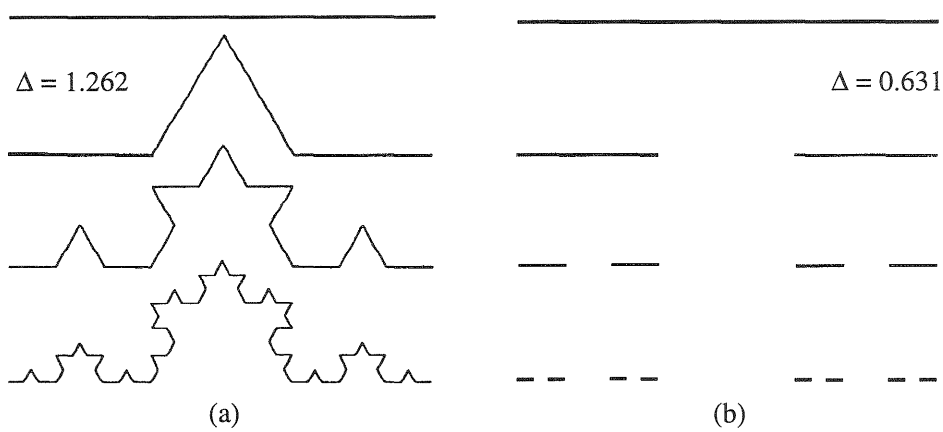

Fig. 3. Invasive (a) and lacunar (b) fractal domains.

In the case of fracture surfaces, *invasive fractals* (i.e. fractal sets with dimension Δ strictly larger than their euclidean projection) are supposed to be adequate models for their topology. The von Koch curve, shown in Fig. 3a, can be considered as the archetype of fracture trajectories obtained as intersections of the fracture surface with orthogonal planes. The space-filling ability of the invasive domains provides *positive scaling exponents* for the mechanical quantities (e.g. the fracture energy) defined over them. On the contrary, the rarefied nature of *lacunar fractals* (like the Cantor set in Fig. 3b), which can be assumed as deterministic models of the damaged material ligament, provides *negative scaling exponents* for the corresponding quantities (e.g. the tensile strength, whose size-dependence has been explained by Carpinteri et al. (1994) as a consequence of lacunar-like disorder).

3 Renormalization group approach to the fracture of concrete

The invasive fractal nature of the fracture surfaces produces a dimensional increment with respect to the number 2. A fractal dimension being non-integer and greater than 2 implies that the dissipation of energy during the fracture process is intermediate between surface energy dissipation (which is the LEFM hypothesis) and volume energy dissipation (which is the approach of Limit Analysis and Damage Mechanics). This agrees with the mean-field definition of $\mathcal{G}_F$ as a product of the *total* work of fracture.

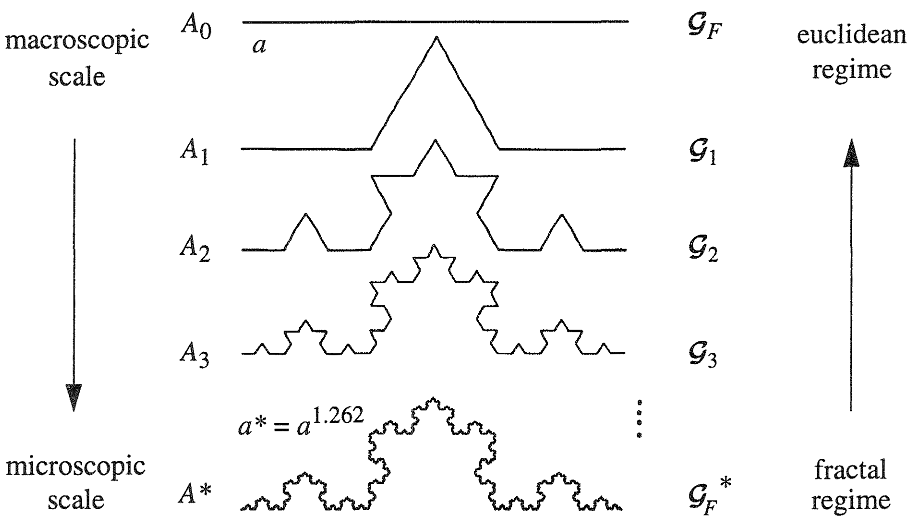

Fig. 4. Renormalization of fracture energy on a fractal domain.

A Renormalization Group (RG) transformation can be applied to the scaling behavior of fracture energy $\mathcal{G}_F$, related to the topological scaling of the dissipation space (Carpinteri, 1994b). For the sake of simplicity, let us model this "surface" by means of a deterministic fractal with dimension $\Delta_{\mathcal{G}}=2+d_{\mathcal{G}}$, whose intersection with an orthogonal plane is a *profile* with dimension equal to $\Delta_{\mathcal{G}}-1$, as shown in Fig. 4. A hierarchical sequence of scales comes into play, where the first scale of observation is the *macroscopic* one (A_0 being the cross-sectional area and $\mathcal{G}_0 = \mathcal{G}_F$ the conventional fracture energy), while the asymptotic scale of observation is the *microscopic* (fractal) one, $A_\infty = A^*$ being the *measure* ($[\mathrm{L}]^{2+d_{\mathcal{G}}}$) of the fractal set , and $\mathcal{G}_F{}^*$ the corresponding *renormalized fracture energy*, defined by the following anomalous dimensions, which are due to the non-integer measurability of fractal sets :

$$\mathcal{G}_F{}^* = [\mathrm{F}]\,[\mathrm{L}]^{-(1+d_{\mathcal{G}})} . \tag{2}$$

A fictitious fracture energy $\mathcal{G}_n$ can be associated to each scale n, which is considered as the energy dissipated at that scale during the formation of the unit crack area. We note that, refining the scale of observation, the energy dissipation involves, at each step, a larger amount of nominal area, ideally tending to infinite in the limit represented by the proper fractal set (E_∞).

On the other hand, the total dissipated energy ΔW is a "macro-parameter", in the sense that it is independent of the observation scale, since it has to satisfy the global energy balance with the critical strain energy release rate. Thus, the following equalities must hold:

$$\Delta W = \mathcal{G}_F A_0 = \mathcal{G}_1 A_1 = \mathcal{G}_2 A_2 = \ldots = \mathcal{G}_F^{\,*} A^* \,. \tag{3}$$

From the definition of Hausdorff measure, if b is a characteristic dimension of the cross-section, the following relations hold:

$$A_0 \approx b^2, \qquad\qquad A^* \approx b^{2+d_{\mathcal{G}}}, \tag{4}$$

and therefore, equating the extreme members of the cascade in Eq. (3), the monofractal scaling relation of the nominal fracture energy is obtained:

$$\mathcal{G}_F \sim \mathcal{G}_F^{\,*} b^{d_{\mathcal{G}}}. \tag{5}$$

Taking the logarithm of both sides of Eq. (5), one obtains:

$$\ln\mathcal{G}_F = \ln\mathcal{G}_F^{\,*} + d_{\mathcal{G}} \ln b, \tag{6}$$

which implies a linear scaling in the bilogarithmic diagram (Fig. 5), representing the *monofractal size effect* on fracture energy.

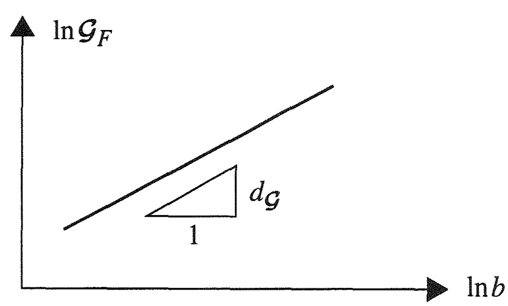

Fig. 5. Monofractal size effect on fracture energy.

The same results can be obtained by extending to fractal crack patterns the Griffith (1921) relation of energy balance, which, at the critical point of unstable crack propagation, states:

$$\frac{\mathrm{d}W_E}{\mathrm{d}a} = \frac{\mathrm{d}W_S}{\mathrm{d}a}, \tag{7}$$

where the first term represents the elastic energy release rate due to the propagation of the pre-existing fractal crack, and $\mathrm{d}W_S$ is the total energy dissipated on the developing fractal crack, due to the breaking of the material bonds and the coalescence of microcracks. The elastic energy release is a macroscopic and global parameter, being it defined in the bulk, which means that it is independent of the observation scale: it is therefore not sensitive to disorder, so that fractality does not come into play in its definition. On the contrary, $\mathrm{d}W_S$ represents the energy directly dissipated in the fractal domain, and thus the *nature* of this dissipation is intimately controlled by the disordered microstructure. Due to the requested dimensional homogeneity in Eq. (7), $\mathrm{d}W_S$ holds the usual dimensions of an energy ([F][L]). In the case of a smooth crack the following relations hold:

$$\frac{\mathrm{d}W_E}{\mathrm{d}a} = \frac{\mathrm{d}}{\mathrm{d}a}\left(\frac{\sigma^2\pi a^2}{E}\right) = \frac{2\pi\sigma^2 a}{E}, \tag{8a}$$

$$\frac{\mathrm{d}W_S}{\mathrm{d}a} = \frac{\mathrm{d}\,(4\gamma a)}{\mathrm{d}a} = 4\gamma = 2\mathcal{G}_F, \tag{8b}$$

where γ ([F][L]$^{-1}$) is the surface energy dissipated on each face of the opening crack. In the presence of a fractal crack, the *renormalized fracture energy* $\mathcal{G}_F^*$ has to be considered as the energy dissipated over the fractal crack. Taking the derivative of a^* with respect to a, where $a^* = a^{(1+d_\mathcal{G})}$ is the *measure* of the fractal profile, leads to simply write:

$$\frac{\mathrm{d}W_S}{\mathrm{d}a} = 2\mathcal{G}_F^*\frac{\mathrm{d}\,(a^*)}{\mathrm{d}a} = 2\,(1+d_\mathcal{G})\,\mathcal{G}_F^*\,a^{d_\mathcal{G}}. \tag{9}$$

A fundamental consequence of the fractality of the fracture surfaces, physically related to the smoothing of the stress-singularity, comes from the comparison between Eqs. (8b) and (9): while, in the case of euclidean cracks, the energy dissipation is independent of a, being constant during crack propagation, in the presence of fractal cracks it increases with a, following a power-law with fractional exponent equal to $d_\mathcal{G}$. If the nominal fracture energy is related to the renormalized one, it is easy to obtain:

$$\mathcal{G}_F \approx \mathcal{G}_F^*\,a^{d_\mathcal{G}}, \tag{10}$$

which clearly indicates that the presence of disorder introduces non-linearity in the fracture behavior of a linear elastic material, thus implying that *the crack resistance grows during the propagation of the fractal crack in an elastic medium* (Fig. 6a) (R-curve behavior).

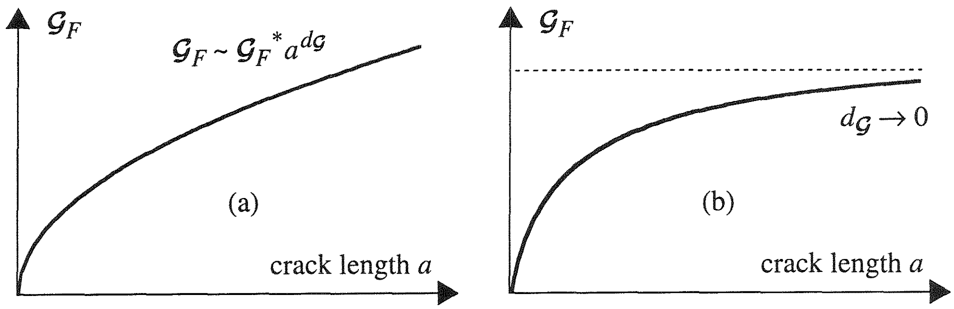

Fig. 6. R-curve behavior. Monofractal (a) and multifractal (b) hypotheses.

4 Multifractal Scaling Law (MFSL) for the nominal fracture energy

As it has been stated in the previous sections, the complexity of the energy dissipation during the fracture process can be consistently synthesized by considering this dissipation to occur in a domain with fractional topological dimension comprised between 2 and 3. In any case, the monofractal scaling behavior described by Eq. (6) and shown in Fig. 5, does not adequately reproduce the experimental results, since an infinite nominal fracture energy would be predicted for the largest sizes, despite an asymptotic constant value of $\mathcal{G}_F$ has always been detected by the tests. Analogously, the crack-resistance behavior provided by Eq. (10) (see Fig. 6a) would yield infinite toughness as the crack extends, which is obviously far from the experimental reality. This is owing to the modelization of the dissipation space by means of a mathematical fractal (a monofractal).

On the contrary, the presence of an *internal characteristic length* l_{ch}, typical of each microstructure, inhibits the development of a perfect self-similar scaling through the whole scale range, whereas mathematical fractals like the von Koch curve in Fig. 4, lacking absolutely of any characteristic length, exhibit uniform (monofractal) scaling without any bound. The topology of the fracture surfaces appears experimentally *multifractal* in the sense that not a unique value of the fractal dimension can be measured, but a continuosly decreasing value with increasing the measurement scale is detected (*geometrical multifractality*), as shown by Carpinteri & Chiaia (1995). The variable fractal dimension, in this context, becomes an indicator of the variable influence of disorder, implying, from the mechanical viewpoint, that *the effect of microstructural disorder on the mechanical properties of the material becomes progressively less important for the larger specimens, whereas it represents the fundamental parameter at the smaller scales* (Carpinteri, 1994b).

Therefore, the relevance of fractality decreases as the crack propagates (that is, as the crack extension a becomes larger and larger with respect to the microstructural characteristic length l_{ch}). It can be affirmed that $d_{\mathcal{G}}$ progressively tends to zero as the crack extends, thus implying, in Eq. (10), an horizontal asymptote for the fracture toughness (Fig. 6b), in perfect agreement with the experimental observations, where a *plateau* in the crack-resistance behavior is always detected. This permits to explain the initial *stable crack growth* that is usually encountered when analyzing the fracture properties of heterogeneous materials.

Extrapolating this constitutive behavior to the problem of the size dependence of $\mathcal{G}_F$ (see Eq. (5)), a transition from a disordered (fractal) regime at the microscopic scales to an euclidean (homogeneous) one at the largest scales is provided in the scaling behavior. The former regime is ideally bounded by a "Brownian" microscopic disorder, corresponding to the highest possible disorder of the fracture domain (local fractal dimension=2.5), whilst the latter regime corresponds to the vanishing of fractality or, which is the same, to the macroscopic homogeneization of the microstructure ($d_{\mathcal{G}} \rightarrow 0$). A strong size-scale effect is provided by the influence of disorder below the transition scale l_{ch}, whereas, beyond l_{ch}, the size effect rapidly vanishes, and the classical euclidean theories (RILEM approach) become applicable since a constant value of the mechanical quantity is attained.

On the basis of these hypotheses, a Multifractal Scaling Law (MFSL) can be deduced for the scaling of the nominal fracture energy, in perfect correspondence with the MFSL already proposed for the nominal tensile strength by Carpinteri et al. (1994). The analytical expression for this Multifractal Scaling Law, represented in Fig. 7a, is the following:

$$\mathcal{G}_F(b) = \mathcal{G}_F^{\infty}\left[1+\frac{l_{ch}}{b}\right]^{-1/2}, \tag{11}$$

where $\mathcal{G}_F^{\infty}$ is the nominal asymptotic fracture energy valid in the limit of infinite structural size ($b \rightarrow \infty$). The non-dimensional term into square brackets represents the decrease, due to the disorder, of the nominal fracture energy with respect to the constant asymptotic value. Note that the asymptotic requirements are satisfied by the former expression: if one takes the derivative of Eq. (11), and takes its limit for $b \rightarrow 0^+$, the maximum slope of the size effect law, equal to +1/2 (Brownian disorder), is obtained.

The horizontal asymptote, corresponding to the larger structural sizes, represents the *homogeneous regime* of the scaling, and is described by the following expression:

$$\ln \mathcal{G}_F = \ln \mathcal{G}_F^{\infty}, \tag{12}$$

whereas the oblique asymptote, corresponding to the *fractal regime* of the scaling, is described by:

$$\ln \mathcal{G}_F = \frac{1}{2}\ln b + \ln\left(\frac{\mathcal{G}_F^{\infty}}{\sqrt{l_{ch}}}\right). \tag{13}$$

Whilst the horizontal asymptote, corresponding to the larger structures, is governed by $\mathcal{G}_F^{\infty}$, which is a purely surface energy, the oblique one, corresponding to the smaller structures, is controlled by the ratio between surface energy and the square root of a length, that is, by a stress-intensity factor (K_I) with physical dimensions [F][L]$^{-3/2}$.

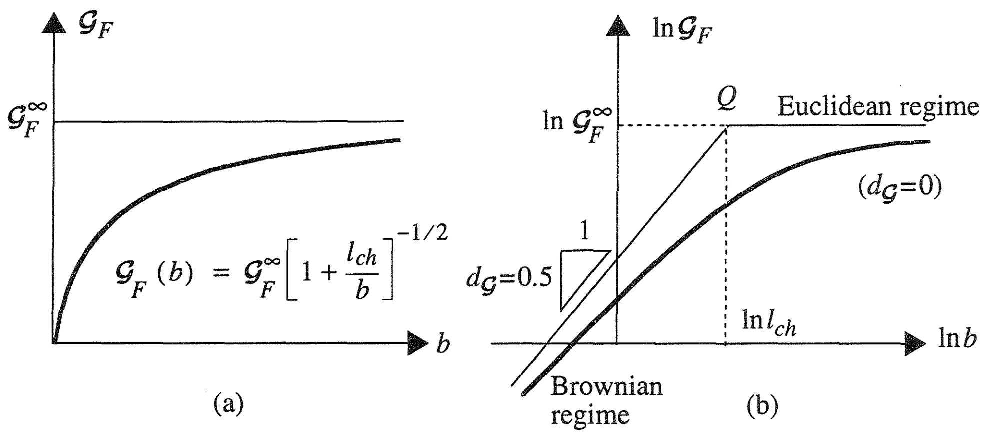

Fig. 7. Multifractal Scaling Law (MFSL) for fracture energy.

On the basis of the MFSL, the RILEM fracture energy, defined as a mean-field quantity, appears to be a physically meaningful parameter only in the homogeneous regime, whereas Linear Elastic Fracture Mechanics, which is characterized by a local approach (K_I), governs the collapse of unnotched structures only when the characteristic size a of microstructural defects becomes comparable with the macroscopic size b of the specimen or, that is the same, when the influence of disorder becomes essential. LEFM always governs the *local* collapse of a material but can be homogeneized in an energy parameter ($\mathcal{G}_F$) only at the larger scales. This is in perfect agreement with the MFSL proposed for tensile strength by the authors, where the Griffith collapse, valid for the smaller sizes, causes the oblique asymptote towards infinite values of strength, whereas a constant (minimum) value of strength can be determined for the larger structures.

The intersection Q between the two asymptotes represents an essential point in the diagram. It is characterized, in fact, by a value of the abscissa equal to the *characteristic length* l_{ch} of the material, which represents a *threshold scale* between the two different scaling regimes, analogously to the case of the MFSL for tensile strength. This internal length, which is a parameter appearing in any sound modelization of heterogeneous materials (non local models, higher order strain gradients, etc.), is typical of any natural fractal domain, whereas mathematical fractals (monofractals) have no characteristic scale and therefore show a linear and unbounded scaling.

It is reasonable to suppose that the value of l_{ch} is related to the size of heterogeneities in the material microstructure, these being the aggregates, in the case of concrete, the grains, in the case of metals, the crystals or the pores, in the case of rocks, the fibers in a fiber-reinforced composite, and even the polymeric chains in a plastic material. In the specific case of concrete, a linear relationship with the maximum aggregate size has been proposed by Carpinteri et al. (1994):

$$l_{ch} = \alpha d_{max}. \tag{14}$$

It can be stated that, in the case of a finer grained mortar, the MFSL is shifted to the left with respect to the case of a coarser concrete mixture, the value of l_{ch} being much lower for the mortar, according to Eq. (14). Generally speaking, one has to determine for each material the proper range of scales where the fractal regime is predominant, and consequently the minimum structural size beyond which the local toughness fluctuations are macroscopically averaged and a constant value of $\mathcal{G}_F$ can be adopted.

5 Analysis of experimental results by means of the MFSL

In this last section, the Multifractal Scaling Law is applied in order to interpretate the results from experimental tests on different concrete geometries. From an engineering point of view, the method allows for the extrapolation, from laboratory-sized specimens, of a reliable value of the fracture energy valid for real-sized concrete structures. The Levenberg-Marquardt algorithm has been implemented in order to fit Eq. (11) to the experimental data, giving as results, for the particular concrete mixture and test geometry considered, the values $\mathcal{G}_F^{\infty}$ and l_{ch}.

The first geometry to be considered is that of Wittmann et al. (1990)

and consists in a series of *compact tests* over a size range 1:4 (b_{min}=150 mm, b_{max}=600 mm, where b is the initial ligament length). The average compression strength f_c is equal to 42.9 MPa, and the maximum aggregate size d_{max} to 16 mm. A two-dimensional similitude is present, the thickness t of the specimens being constanly equal to 120 mm. Six specimens have been tested for each representative size. The nominal values of the fracture energy are obtained by the ratio between the total work of fracture (area under the load-displacement curve) and the initial area of the ligament ($b \times t$). Note that the authors cut the end of the softening tail, intending that the *hinge-mechanism* due to bridging and interlocking between aggregates has not to be taken into account in the toughness evaluation.

The application of the MFSL to the $\mathcal{G}_F$ values is shown in Fig. 8a. The asymptotic fracture energy results $\mathcal{G}_F^{\infty}$ = 196.2 N/m, and the characteristic internal length l_{ch}=209.5 mm. Therefore, the asymptotic toughness is about the 40% larger than the smallest specimens' value (121.5 N/m). On the basis of Eq. (14), the non-dimensional parameter α results equal to 13.1. The correlation coefficient, which is a clue for the *goodness of fit*, turns out to be R=0.937.

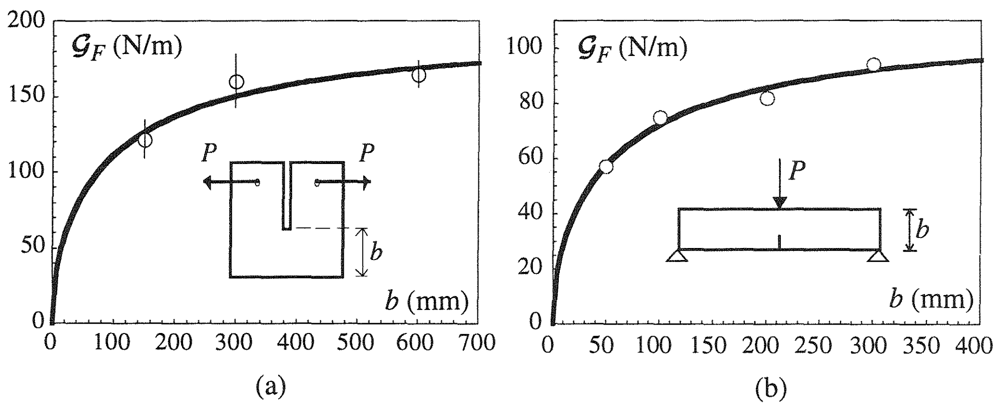

Fig. 8. Application of the MFSL to the data by Wittmann et al. (a) and to the data by Elices et al. (b).

Experimental results obtained by rigorously following the RILEM Recommendation are those by Elices et al. (1992). Three-point bending tests under crack opening control have been carried out by the authors on beams made of concrete with d_{max}= 10 mm and f_c=33.1 MPa. As in the previous case, only a two-dimensional similitude is provided, the thickness t being equal to 100 mm for all the beams. The beam height, assumed as the reference size, ranges from 50 mm to 300 mm (range 1:6). The nominal fracture energy is obtained from the total work of fracture (considering also the weight of the beam and of the testing equipment), divided by the initial ligament ($(b-a_0)\times t$, where $a_0=b/3$ is the initial notch depth). The application of the MFSL is shown in Fig. 8b: the best-fitting values are respectively $\mathcal{G}_F^{\infty}=110.6$ N/m and $l_{ch}=133.1$ mm. The asymptotic fracture energy is therefore almost 90% larger than the smallest specimens' value (57 N/m). The non-dimensional parameter $\alpha=l_{ch}/d_{max}$ is equal to 13.3, whilst the correlation coefficient turns out to be $R=0.982$.

An innovative test procedure has been recently developed by Carpinteri & Ferro (1994) in order to determine the tensile properties of concrete. *Bone-shaped* specimens, bounded with fixed plates at their ends, are tested in direct tension, under displacement controlled loading. The use of three independent jacks, the first one acting axially, the others on the two principal planes, compensates the load eccentricities due to the not uniform damage through the reacting ligament. Therefore, no bending moment is present during the loading process. A larger fracture energy, with respect to three-point bending specimens, is obtained from these tests: this is due to the (infinite) stiffness of the boundary conditions, which may give rise to the formation of two macrocracks instead of one as in the RILEM test, and to their subsequent bridging, thus resulting in a long-tail softening. The maximum aggregate size is $d_{max}=16$ mm, and the average compressive strength is equal to 36.9 MPa. A two-dimensional similitude is present, the thickness t of the *"bones"* being constantly equal to 100 mm. A 1:8 size interval has been tested, ranging from $b=50$ mm to 400 mm, b being the width at the neck of the specimens.

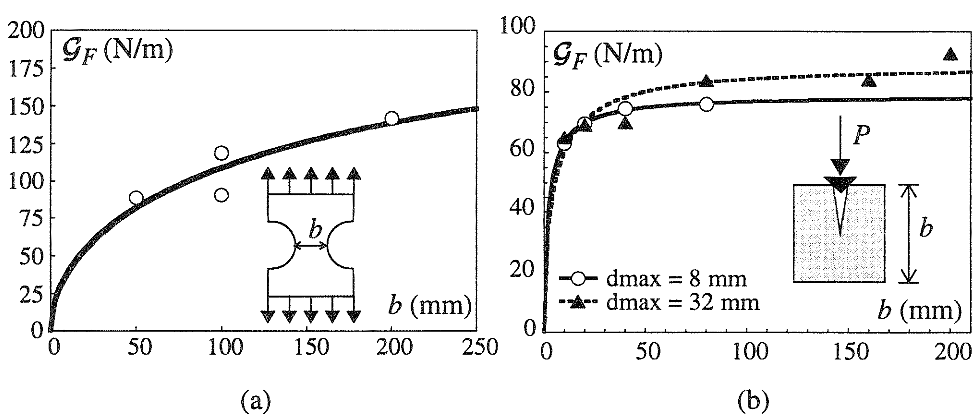

Fig. 9. Application of the MFSL to the data by Carpinteri & Ferro (a) and to the data by Zhong (b).

The application of the MFSL is shown in Fig. 9a: the asymptotic fracture energy results $\mathcal{G}_F^\infty$=226.4 N/m, and the characteristic internal length l_{ch}=328.8 mm. The non-dimensional parameter α results equal to 20.5 and the correlation coefficient R to 0.864.

Zhong (1991) performed wedge-splitting tests on two series of concrete with different maximum grain size, 8 mm and 32 mm respectively. The examined size range is equal to 1:8 in the case of the finer mixture and to 1:20 in the case of the coarse one. In Fig. 9b the application of the MFSL to the experimental data is shown: in the case of the finer grained concrete, non linear fitting yields the asymptotic fracture energy $\mathcal{G}_F^\infty$=78.9 N/m, and the characteristic internal length l_{ch}=5.6 mm (α=0.7), whereas, in the case of the coarse grained concrete, the following parameters are determined: $\mathcal{G}_F^\infty$=89.1 N/m and l_{ch}=11.8 mm (α=0.37). The correlation coefficient R results equal to 0.997 and to 0.881, for the finer and the coarser mix respectively. As expected, concrete with a larger maximum aggregate size has a higher asymptotic fracture energy. Moreover, it is interesting to point out that the coarse mixture yields a larger internal length, according to the MFSL, and therefore the transition to the homogeneous behavior occurs later than in the case of the 8 mm mixture. It is therefore confirmed that the value of l_{ch} is intimately related to the maximum aggregate size, as previously supposed by the authors.

6 References

Carpinteri, A. (1994a) Fractal nature of material microstructure and size effects on apparent mechanical properties. **Mechanics of Materials**, 18, 89-101.

Carpinteri, A. (1994b) Scaling laws and renormalization groups for strength and toughness of disordered materials. **International Journal of Solids and Structures**, 31, 291-302.

Carpinteri, A. & Chiaia, B. (1995) Multifractal nature of concrete fracture surfaces and size effects on nominal fracture energy. In press on **Materials and Structures**.

Carpinteri, A., Chiaia, B. and Ferro, G. (1994) Multifractal nature of material microstructure and size effects on nominal tensile strength. In **Proc. of the IUTAM Symposium on Fracture of Brittle Disordered Materials: Concrete, Rock & Ceramics**, (Baker, G. & Karihaloo, B.L. eds.), E. & F.N. Spon, London, 21-34.

Carpinteri, A. & Ferro, G. (1994) Size effects on tensile fracture properties: a unified explanation based on disorder and fractality of concrete microstructure. **Materials and Structures**, 27, 563-571.

Elices, M., Guinea, G.V. and Planas, J. (1992) Measurement of the fracture energy using three-point bend tests: Part 3 –Influence of cutting the P–δ tail. **Materials and Structures**, 25, 327-334.

Griffith, A.A. (1921) The phenomenon of rupture and flow in solids. **Philosophical Transaction of the Royal Society**, A221, London, 163-198.

Hillerborg, A., Modeer, M. and Petersson, P.E. (1976) Analysis of crack formation and crack growth in concrete by means of fracture mechanics and finite elements. **Cement and Concrete Research**, 6, 773-782.

Hillerborg, A. (1985) Results of three comparative test series for determining the fracture energy $\mathcal{G}_F$ of concrete. **Materials and Structures**, 18, 407-413.

Hu, X.Z. & Wittmann, F.H. (1992) Fracture energy and fracture process zone. **Materials and Structures**, 25, 319-326.

Issa, M.A. & Hammad, A.M. (1994) Assessment and evaluation of fractal dimension of concrete fracture surface digitized images. **Cement and Concrete Research**, 24, 325-334.

Lange, D.A., Jennings, H.M. and Shah, S.P. (1993) Relationship between fracture surface roughness and fracture behavior of cement paste and mortar. **Journ. Amer. Ceram. Soc.**, 76, 589-597.

RILEM Technical Committee 50 (1985) Determination of the fracture energy of mortar and concrete by means of three-point bend tests on notched beams. Draft Recommendation. **Materials and Structures**, 18, 287-290.

Saouma, V.E., Barton, C.C. and Gamaleldin, N.A. (1990) Fractal characterization of fracture surfaces in concrete. **Engineering Fracture Mechanics**, 35, 47-53.

Schlangen, E. (1995) Computational aspects of fracture simulations with lattice models. **These Proceedings**.

Swartz, S.E. & Refai, T.M.E. (1987) Influence of size effects on opening mode fracture parameters for precracked concrete beams in bending. In **Proc. of the SEM/RILEM Int. Conf. Fracture of Concrete and Rock** (Shah, S.P. and Swartz, S.E. eds.), Houston, 403-417.

Wittmann, F.H., Mihashi, H. and Nomura, N. (1990) Size effect on fracture energy of concrete. **Engineering Fracture Mechanics**, 35, 107-115.

Zhong, H. (1991) Some experiments to study the influence of size and strength on fracture energy. **Internal Report of the Institute for Building Materials**, Swiss Federal Institute of Technology, Zürich.